

- ¹See, for example, R. L. Aggarwal, F. Fisher, V. Mourzive, and A. K. Ramdas, *Phys. Rev.* **138**, A882 (1965).
- ²D. G. Thomas, M. Gershenzon, and F. A. Trumbore, *Phys. Rev.* **133**, A269 (1964).
- ³F. A. Trumbore and D. G. Thomas, *Phys. Rev.* **137**, 1030 (1965).
- ⁴P. J. Dean, C. H. Henry, and C. J. Frosch, *Phys. Rev.* **168**, 812 (1968).
- ⁵P. J. Dean, C. J. Frosch, and C. H. Henry, *J. Appl. Phys.* **39**, 5631 (1968).
- ⁶P. J. Dean, J. D. Cuthbert, D. G. Thomas, and R. T. Lynch, *Phys. Rev. Letters* **18**, 122 (1967).
- ⁷P. J. Dean, J. R. Haynes, and W. F. Flood, *Phys. Rev.* **188**, 711 (1969).
- ⁸D. C. Reynolds, C. W. Litton, and T. C. Collins, *Phys. Rev.* **174**, 845 (1968).
- ⁹D. C. Reynolds, C. W. Litton, and T. C. Collins, *Phys. Rev.* **177**, 1161 (1969).
- ¹⁰D. C. Reynolds and T. C. Collins, *Phys. Rev.* **185**, 1099 (1969).
- ¹¹C. H. Henry, J. J. Hopfield, and D. G. Thomas, *Phys. Rev.* **17**, 1178 (1966).
- ¹²G. B. Wright and A. Mooradian, in *Proceedings of the Ninth International Conference on the Physics of Semiconductors*, edited by S. M. Ryvkin (Nauka, Leningrad, 1968), p. 1067; *Phys. Rev. Letters* **18**, 608 (1967).
- ¹³J. J. Hopfield and D. G. Thomas, *Phys. Rev.* **122**, 35 (1961).
- ¹⁴D. G. Thomas and J. J. Hopfield, *Phys. Rev.* **128**, 2135 (1962).
- ¹⁵E. T. Handelman and D. G. Thomas, *J. Phys. Chem. Solids* **26**, 1261 (1965).
- ¹⁶R. G. Wheeler and J. O. Dimmock, *Phys. Rev.* **125**, 1805 (1962).
- ¹⁷C. H. Henry and K. Nassau, *Phys. Rev. B* **1**, 1628 (1970).
- ¹⁸J. J. Hopfield, in *Proceedings of the Seventh International Conference on the Physics of Semiconductors, Paris, 1964* (Academic, New York, 1965), p. 725.
- ¹⁹D. C. Reynolds, C. W. Litton, and T. C. Collins, *Proc. Roy. Soc. (London)* (to be published).
- ²⁰D. G. Thomas and J. J. Hopfield, *Phys. Rev.* **175**, 1021 (1968).
- ²¹A. S. Barker and C. J. Summers (unpublished).
- ²²A. R. Hutson, *J. Appl. Phys. Suppl.* **32**, 2287 (1961).
- ²³G. Vella-Coleiro, *Phys. Rev. Letters* **23**, 697 (1969).
- ²⁴W. W. Piper and R. E. Halsted, in *Proceedings of the International Conference on Semiconductor Physics, Prague, 1960* (Academic, New York, 1961), p. 1046.

Electric-Susceptibility Mass of Free Holes in SnTe[†]

R. F. Bis and J. R. Dixon

U.S. Naval Ordnance Laboratory, White Oak, Silver Spring, Maryland 20910
and

University of Maryland, College Park, Maryland 20740

(Received 9 September 1969; revised manuscript received 4 March 1970)

The electric-susceptibility mass m_s of free carriers was determined at 300, 80, and 10°K for *p*-type SnTe having carrier concentrations ranging from 3.6×10^{19} to 1.2×10^{21} cm⁻³. The values were determined from an analysis of the normal reflectivity of the material in the infrared region. The observed carrier concentration and temperature dependences of m_s were used to test valence-band models recently proposed for SnTe by (i) Koehler, (ii) Rogers, and (iii) Tsu, Howard, and Esaki. In addition, a simple Cohen-type model was evaluated. It is demonstrated that none of these models provides a completely satisfactory description of our experimental results. The temperature dependence of m_s is shown to be anomalous with regard to its relationship to the temperature dependence of the forbidden energy gap. On the basis of our results, it is concluded that the valence-band structure of SnTe is considerably more complex than indicated by the models we have considered.

I. INTRODUCTION

Recently, a considerable amount of research has been directed toward an understanding of the valence-band structure of SnTe.¹⁻⁴ Despite this effort, the nature of this structure has not yet been delineated. Furthermore, a number of mutually inconsistent valence-band models have been proposed for this material.²⁻⁴ An objective of the

work which we report here was to test these band models by experimentally determining the electric-susceptibility mass m_s as a function of temperature and carrier concentration. Measurements of m_s are particularly useful for this purpose, because they are sensitive to the nature of the contributing bands at the Fermi level. Since the position of the Fermi level can be changed by varying the carrier concentration, various parts of the band

structure can be probed. Another appealing aspect of such measurements is that they can be carried out over unusually large ranges of temperature and carrier concentration. For example, our studies involved a range of temperatures from 10 to 300°K and hole concentrations from 3.6×10^{19} to $1.2 \times 10^{21} \text{ cm}^{-3}$.

Previous measurements of m_s at 300°K showed that it was a strong function of carrier concentration, indicating some combination of nonparabolic and multiple valence-band structures.⁵ Our range of carrier concentrations and temperatures represents an extension of these data to lower temperatures and to both lower and higher carrier concentrations. We have compared the results of these measurements with those expected on the basis of the previously proposed band models, as well as for a simple one-band Cohen-type model. In addition, on the basis of our measurements we have found an anomalous relationship between the temperature dependence of m_s and the corresponding variation of the forbidden energy gap. Finally, the relevance of these results to current band-structure considerations is discussed.

II. EXPERIMENTAL

A. Bulk Samples

Four bulk single crystals of SnTe were studied. They were grown by Houston *et al.*⁶ of our laboratory. Circular disks having diameters of approximately $\frac{1}{2}$ in. and thicknesses of $\frac{1}{8}$ in. were cut from these single crystals. Using a technique similar to that of Brebrick,⁷ Houston heat treated these crystals to vary their hole concentration from their as-grown value of approximately $5 \times 10^{20} \text{ cm}^{-3}$.

Values of the hole concentration p were determined from measurements of the weak-field Hall coefficient R_H and the relation $p = (r/R_H e)_{277^\circ \text{K}}$. In doing this we have employed a value of 0.6 for the anisotropy factor r .⁸ The carrier concentrations of our samples obtained in this way are presented in Table I.

Sample surfaces were prepared for reflectivity measurements by polishing and etching, using a procedure and etch developed by Norr.⁹ Our reflectivity measurements were dependent upon the nature of a thin surface layer, the optical penetration depth being about 1μ . For this reason we have examined the crystallographic condition of this layer using x rays. Laue photographs were taken under conditions which minimized the x-ray penetration depth. This involved low x-ray tube voltages, an iron target, and long exposures of approximately 5 h. Under these conditions the penetration depth of the x rays approximated the optical penetration depth. The Laue photographs

TABLE I. Carrier concentrations of SnTe samples.

| Sample | Type | Carrier concentration ^a (cm^{-3}) |
|--------|------|--|
| A | Bulk | 1.38×10^{20} |
| B | Bulk | 2.95×10^{20} |
| C | Bulk | 5.30×10^{20} |
| D | Bulk | 1.20×10^{21} |
| E | Film | 3.60×10^{19} |
| F | Film | 7.50×10^{19} |
| G | Film | 1.40×10^{20} |

^aAll samples are p type.

taken under the above conditions had sharp spots characteristic of good single-crystal material. Therefore, we believe that the surface layer involved in the optical measurements was free of major damage and strains.

Reflectivity measurements at near-normal incidence were made in the infrared using a Perkin-Elmer Model 112 spectrometer equipped with either a LiF or a NaCl prism. A standard optical Dewar was used to achieve sample temperatures of 300, 80, and 10°K. The reflectometer¹⁰ was similar to that developed by Paul and his associates at Harvard University. A particularly appealing characteristic of this system is that it produces a narrow beam of light, permitting entry into the Dewar without vignetting. A 1:1 image of the exit slit of the monochromator is formed on the sample. The angle of incidence of the central ray upon the sample is about 10° from normal, while that of the extreme rays is approximately 15°. These angles are sufficiently small so that the measurements correspond to within 1% of those at normal incidence. The reflectivity was determined by comparing the light reflected from the sample with that from a standard front-surfaced aluminum mirror.

B. Film Samples

Film samples deposited epitaxially on NaCl substrates were studied in addition to bulk samples because relatively small hole concentrations could be more readily obtained by heat treatment of the films. This was true because the thinness of the films (approximately 1μ) greatly reduced the time required to complete the diffusion process involved in the heat treatment.¹¹ The films were single crystals having areas of approximately 1 cm^2 and the hole concentrations given in Table I. These hole concentrations were determined in the manner described above for the case of bulk samples. Reflectance measurements at near-normal incidence were made on these films using a Perkin-Elmer

Model 21 spectrometer with a reflectance attachment placed in the entrance optics. A standard front-surfaced aluminum mirror was used for reference. The fringe data obtained on the SnTe film samples were similar to those reported by Riedl *et al.*¹¹

III. DISPERSION THEORY

The reflectivity R at normal incidence is given in terms of the index of refraction n and the extinction coefficient k by

$$R = [(n-1)^2 + k^2] / [(n+1)^2 + k^2]. \quad (1)$$

It is related to the complex dielectric constant $\tilde{\epsilon}$ through the defining relations

$$\tilde{\epsilon} = \epsilon_1 + i\epsilon_2 = n^2 - k^2 + 2ink. \quad (2)$$

The frequency dependence of this dielectric constant arises principally from three dispersion mechanisms involving bound carriers (BC), free carriers (FC), and lattice vibrations (LV). It is usually assumed that their contributions to $\tilde{\epsilon}$ are additive, as expressed by

$$\tilde{\epsilon} = \tilde{\epsilon}_{BC} + \tilde{\epsilon}_{FC} + \tilde{\epsilon}_{LV} = 1 + 4\pi(\tilde{\chi}_{BC} + \tilde{\chi}_{FC} + \tilde{\chi}_{LV}). \quad (3)$$

The $\tilde{\chi}$'s are the electric susceptibilities corresponding to each mechanism.

In the spectral region from 1 to 15 μ , which was studied here, $\tilde{\chi}_{LV}$ makes a relatively small contribution to $\tilde{\epsilon}$. In addition, at wavelengths somewhat beyond the fundamental absorption edge, $\tilde{\chi}_{BC}$ becomes independent of wavelength. When these conditions are satisfied, Eq. (3) is customarily written as

$$\tilde{\epsilon} = \epsilon_\infty + 4\pi\tilde{\chi}_{FC}, \quad (4)$$

where ϵ_∞ is the optical dielectric constant.¹² According to classical dispersion theory, $\tilde{\chi}_{FC}$ is related to the free carrier concentration N , electric-susceptibility mass m_s , and damping coefficient γ by

$$\tilde{\chi}_{FC} = (-Ne^2/m_s)[1/(\omega^2 + \gamma^2)](1 - i\gamma/\omega), \quad (5)$$

where ω is the angular frequency of the light and e is the electronic charge. This expression is in cgs units.

Another quantity of interest is the optical mobility μ_{opt} , which we define as

$$\mu_{opt} \equiv e/m_s\gamma. \quad (6)$$

It follows directly from Eqs. (1)–(6) that R may be expressed in functional form as

$$R = R(N, m_s, \epsilon_\infty, \mu_{opt}, \omega). \quad (7)$$

Since N is determined by an independent measurement and ω is controlled, this functional relation for R involves three unknown quantities. We have

analyzed our experimental data to obtain values for these parameters.

IV. RESULTS AND DISCUSSION

A. Reflectivity of Bulk Samples

Reflectivity data which apply to the four bulk samples are presented in Fig. 1. These data represent extensions of previously reported data⁵ to lower temperatures and to higher carrier concentrations. The solid curves were calculated on the basis of the free carrier dispersion relations described above and the parameters indicated in the figure. The calculated curves are in good agreement with the experimental data at wavelengths greater than approximately 3 μ . The discrepancies at shorter wavelengths are due to the onset of bound carrier dispersion. Such discrepancies have been discussed in detail by Riedl *et al.*,⁵ and Schoolar *et al.*^{13,14} In addition, small discrepancies of less than 5% occur on the long-wavelength side of the reflectivity minimum for samples of high carrier concentration. Fortunately, the determination of m_s , the parameter of primary interest here, was relatively insensitive to the reflectivities in the long-wavelength region. For this reason, we have not carried out a systematic study to determine the origin of the long-wavelength discrepancy.

B. Reflectance of Thin Film Samples

Three film samples were studied at 300 and 80°K using a procedure described by Schoolar and Dixon¹⁴ and Riedl and Schoolar.¹⁵ This involved measuring the wavelength λ at which maximum and minimum reflectances occur. Since the thicknesses of the films were known,^{14,16} the positions of the maxima and minima gave the index of refraction directly. The preceding assertion is true providing $n \gg k$. It has been shown by previous detailed optical studies^{5,14,15} that this condition is satisfied in the spectral region of our measurements for films of the type studied here. If in addition $\omega^2 \gg \gamma^2$, it follows from Eqs. (2) and (5) that

$$n^2 = \epsilon_\infty - (e^2/\pi c^2)(N/m_s)\lambda^2, \quad (8)$$

where c is the velocity of light. Thus, under these conditions a plot of n^2 versus λ^2 serves to establish ϵ_∞ and m_s . The validity of applying Eq. (8) to the analysis of our data was supported by the fact that a λ^2 dependence for n was observed experimentally. The values of m_s and ϵ_∞ reported for the film samples were obtained in this manner.

The reliability of our film data is supported also by the close agreement of the dispersion parameters obtained for a film and a bulk sample

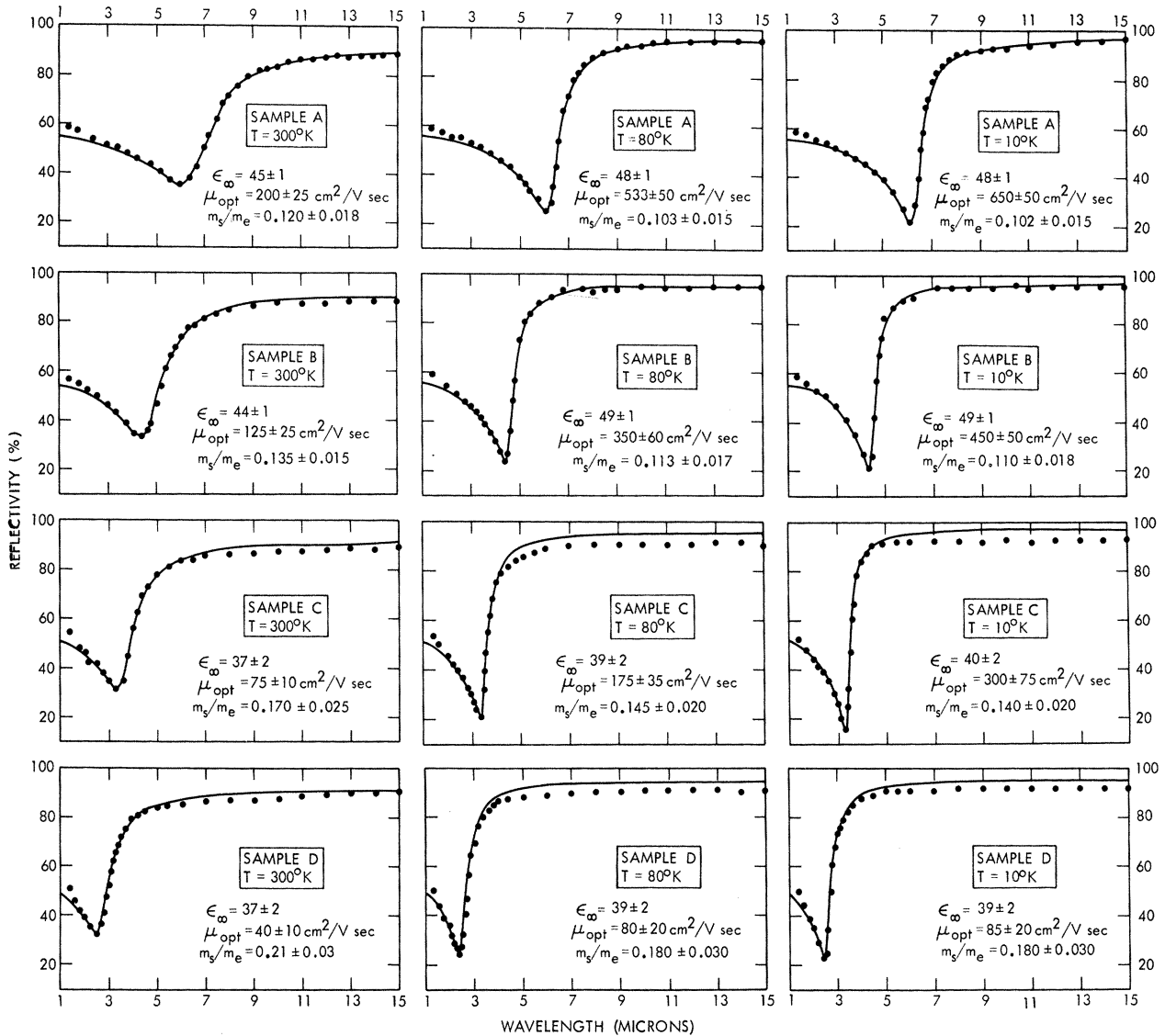


FIG. 1. Reflectivity spectra at 300, 80, and 10°K for samples A–D. Samples are described in Table I. Solid curves represent values calculated on the basis of classical free carrier dispersion theory, as discussed in the text. The dispersion parameters used in these calculations are given in the lower right-hand corner of each figure.

having similar carrier concentrations. The samples involved were samples A and G. As indicated above, the methods of analysis were completely different in the two cases. The fact that the same dispersion parameters were obtained for each type of sample at both 300 and 80°K serves as evidence supporting both methods of analysis.

C. Dispersion Parameters

The dispersion parameters resulting from analyzing our bulk and thin film data as discussed above are presented in Fig. 1 and Table II, re-

spectively.

The values of ϵ_∞ , μ_{opt} , and m_s at 300°K are in good agreement with those previously reported.^{5,15}

The values of ϵ_∞ presented in Table II and Fig. 1 increase as the carrier concentration decreases. This type of dependence has been observed previously for SnTe and is attributed at least partially to a Burstein shift¹⁷ of the fundamental absorption edge.^{13,14} In addition, ϵ_∞ increases with decreasing temperature. A similar dependence has been observed for PbTe¹⁸ and PbS^{15,19} and is presumably due to the temperature-dependent

TABLE II. Optical dispersion parameters - film samples.

| Sample | Temperature (°K) | ϵ_∞ | m_s/m_e |
|--------|------------------|-------------------|---------------|
| E | 300 | 48 ± 2 | 0.075 ± 0.018 |
| | 80 | 54 ± 2 | 0.056 ± 0.018 |
| F | 300 | 45 ± 2 | 0.100 ± 0.012 |
| | 80 | 51 ± 2 | 0.070 ± 0.010 |
| G | 300 | 45 ± 2 | 0.120 ± 0.020 |
| | 80 | 47 ± 2 | 0.100 ± 0.011 |

shifts of the electronic energy bands.

Our primary interest was the experimental determination of m_s . Its variation with carrier concentration is presented in Fig. 2 at 300 and 80°K. The 10°K results are not presented as they are essentially the same as the 80°K results. It can be seen in Fig. 2 that m_s increases as the carrier concentration increases, and decreases by about 20% in going from 300 to 80°K at all carrier concentrations.

D. Influence of Multiple Bands upon Dispersion

Many of the models which have been proposed to explain various electrical, optical, and thermal properties of SnTe have involved multiple valence bands. The use of single-band dispersion theory, as we have done, to analyze a multiple-band situation would be expected, in general, to lead to sizable errors in the evaluation of band parameters such as m_s . This point has not been taken into account in previous work²⁻⁵ of this nature on SnTe. Consequently, the meaningfulness of earlier band models arrived at by comparison with m_s data must be considered uncertain at this point.

The complexities referred to above can be appreciated by considering the classical dispersion relation applying to a multiple-band system¹²

$$\epsilon = \epsilon_\infty - 4\pi e^2 \sum_j \frac{N_j}{m_{s,j}} \left(\frac{1}{\omega^2 + \gamma_j^2} \right) \left(1 - \frac{i\gamma_j}{\omega} \right), \quad (9)$$

where j is the band index. This relation is analogous to Eqs. (4) and (5) for the single-band situation. Thus, when the possibility of multiple bands exists, considerable care must be exercised in order to extract meaningful band parameters from the optical data.

For the reasons given above, the exceptionally good agreement between our reflectivity data and the results calculated on the basis of single-band dispersion theory would not be expected generally. The fact that good fits are obtained with the single-band relation suggests one of two possibilities: (a) Multiple valence bands are not involved, and only a single type of valence band is actually oc-

cupied by the free carriers. (b) Multiple valence bands are involved, but the dispersion parameters associated with each of the bands are such that Eq. (9) takes on the form of the single-band relation of Eq. (4). Because of the rather strong evidence supporting the existence of multiple valence bands, we believe that the latter possibility is the more likely one. This belief is supported by the fact that the second situation is realized providing the damping coefficients associated with each band are such that

$$\gamma_1^2, \gamma_2^2, \gamma_3^2, \dots \ll \omega^2. \quad (10)$$

Estimates based upon the carrier scattering mechanisms believed to be active in this material indicate that this condition is not unrealistic.

V. COMPARISON OF EXPERIMENT WITH VARIOUS BAND MODELS

A. Carrier Concentration Dependence

1. Koehler Model

Recently, Koehler² proposed a multiple valence-band model to explain the optical and thermal properties of SnTe. The model consists of two spherical valence bands whose extrema are separated by 0.29 eV. The upper band involved four equivalent energy surfaces in the $\langle 111 \rangle$ directions. It was assumed to be parabolic to an energy of 0.29 eV and to become appreciably nonparabolic

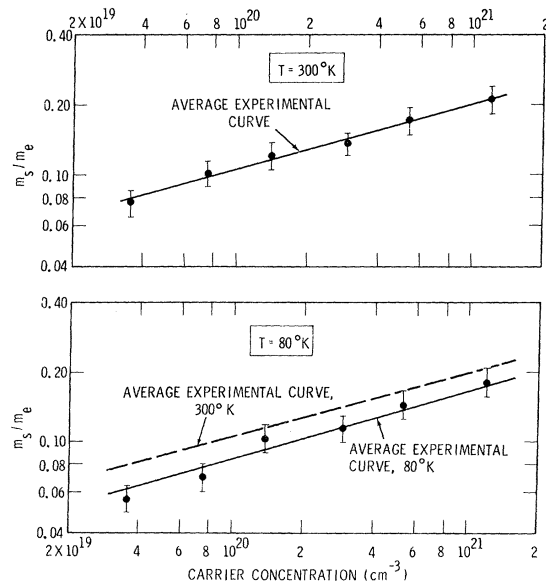


FIG. 2. Variation of the electric susceptibility hole mass m_s/m_e with carrier concentration at 300 and 80°K. The 80°K results are about 20% below those at 300°K at all carrier concentrations.

at higher energies. The six energy surfaces associated with the second band were situated along the $\langle 110 \rangle$ directions and were taken to be parabolic. We have calculated the variation of m_s with carrier concentration which would be expected on the basis of such a model. In carrying out this calculation, we used Koehler's values of the Hall coefficient obtained only at 300°K to estimate the corresponding values at 77°K. This was done to permit a direct comparison of his carrier concentrations [calculated from $(R_H)_{300^\circ\text{K}}$] with ours [calculated from $(R_H)_{77^\circ\text{K}}$]. The adjustments were based upon the values of $(R_H)_{300^\circ\text{K}}/(R_H)_{77^\circ\text{K}}$ reported by Houston and Allgaier²⁰ and our relation for p given in Sec. IIA. The results are presented as the solid curve in Fig. 3. They are characterized by an m_s which is essentially constant until the Fermi level enters the second band, and then by an increasing m_s at higher carrier concentrations. It can be seen that the calculated curve is in marked disagreement with our experimental results over the whole range of carrier concentrations. Thus, it appears that the Koehler model does not provide a suitable description of our experimental results.

2. Rogers Model

Rogers³ proposed a two-valence-band model to explain the electrical, optical, and thermal properties of SnTe. The energy surfaces associated with the upper band were taken to be the nonparabolic approximately ellipsoidal surfaces first described by Cohen.²¹ The extrema of these surfaces were placed at the edges of the Brillouin zone in the $\langle 111 \rangle$ directions. The second band was taken to be parabolic, and its twelve equivalent surfaces were located in the interior of the Brillouin zone along the $\langle 110 \rangle$ directions. The extrema of the two bands were separated by approximately 0.3 eV.

As part of his analysis, Rogers calculated the electric-susceptibility mass to be expected on the basis of his model at two carrier concentrations. In carrying out these calculations, Rogers first determined the band parameters of the Cohen-type surfaces at the two carrier concentrations, and then substituted these parameters into the standard relation for parabolic ellipsoids. Because of this latter step, we consider his analysis as a partial treatment of m_s for the Cohen surfaces. As we shall show, such a partial treatment introduces a significant error into the calculated values of m_s . Rogers's values for m_s are plotted as the X's in Fig. 4. In doing this we have adjusted Rogers's carrier concentrations [based upon $(R_H)_{300^\circ\text{K}}$] so as to correspond to ours, as described in Sec. VA. The results of Rogers's partial treatment give an

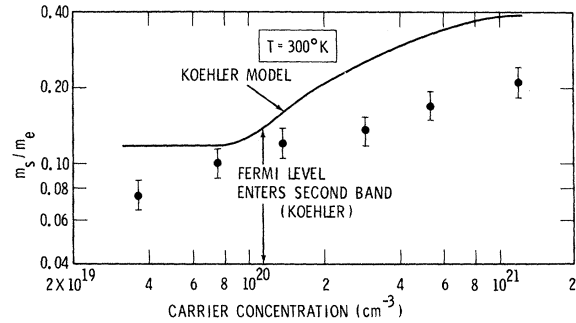


FIG. 3. Comparison of the experimental carrier concentration dependence of the electric-susceptibility hole mass m_s/m_e at 300°K with that expected on the basis of the Koehler model.

m_s which is somewhat larger than our experimental value at both carrier concentrations.

In addition, we have carried out the more desirable full treatment of the Cohen surfaces. This was done using Rogers's band parameters and the equations for m_s of a Cohen surface developed by Dixon and Riedl.¹⁸ The results of this calculation are presented as the solid curve in Fig. 4. These calculated values of m_s are considerably larger than the experimental ones at all carrier concentrations. Therefore, it appears that the band model proposed by Rogers for SnTe also leads to an m_s which is not consistent with our experimental data.

3. Tsu, Howard, and Esaki Model

Tsu, Howard, and Esaki⁴ (THE) have also proposed a two-valence-band model to explain the electrical and optical properties of SnTe. The energy surfaces associated with the upper band were taken to be Cohen-like. As before, the extremum of this band was placed at the edges of the Brillouin zone in the $\langle 111 \rangle$ directions. The energy surfaces associated with the second band were taken to be parabolic and were also placed at the edges of the Brillouin zone in the $\langle 111 \rangle$ directions. The extrema of the two bands were separated by 0.34 eV at 300°K.

The essential differences between the work of THE and that of Rogers are (a) THE performed the more desirable full treatment of the Cohen surface in the calculation of m_s , as compared to Rogers's partial treatment; (b) Rogers and THE located the extrema associated with their second bands at different places in the Brillouin zone; (c) THE proposed a light-hole second band, whereas Rogers proposed a heavy-hole second valence band. Using their model, THE calculated the carrier dependence of m_s at 300°K and fit the re-

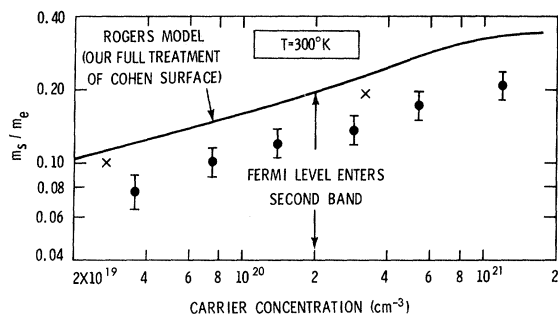


FIG. 4. Comparison of the experimental carrier concentration dependence of the electric-susceptibility hole mass m_s/m_e at 300°K with that expected on the basis of the Rogers model. The X⁷ represent Rogers's calculation. Solid curve represents our extension of Rogers model to a full treatment of the Cohen surface, as discussed in the text.

sults to their experimental data as well as to that of Riedl *et al.*⁵ Their calculations are presented as the solid curve in Fig. 5. The dashed curve represents our extension of their calculations. The calculated curve is in good agreement with the data in the low carrier concentration range, but a significant discrepancy exists above a carrier concentration of about $4 \times 10^{20} \text{ cm}^{-3}$. This discrepancy is not large enough, however, to serve as definite grounds for ruling out this model. Of the three models we have considered, it provides by far the most satisfactory description of the carrier concentration dependence of m_s at 300°K.

4. Simple Cohen-Type Model

Our experimental results at 300°K can be described by a relatively simple model, involving only a Cohen-type valence band acting alone. To

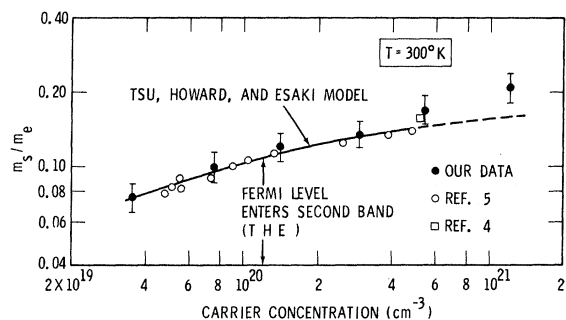


FIG. 5. Comparison of the experimental carrier concentration dependence of the electric-susceptibility hole mass m_s/m_e , at 300°K with that expected on the basis of the THE model. The broken curve represents our extension of the THE calculation as discussed in the text. Other experimental data have been included for comparison.

demonstrate this, we have calculated the carrier concentration dependence of m_s at 300°K based upon such a model. In carrying out this calculation, we have used the method described by Dixon and Riedl¹⁸ and the band parameters given by THE.

The results of our calculation are presented in Fig. 6 as the solid curve. They are in better agreement with our experimental results than the calculations of THE which include the influence of a second band. However, this good agreement should not be considered necessarily as strong supporting evidence for our simple model. This limitation arises because of uncertainties which exist in the determination of the hole concentration p and, consequently, in the determination of m_s . Our experimental method of determining the number of carriers in the Cohen surfaces from measurements of the weak-field Hall coefficient R_H differs, for example, from that which would have been used by THE for this single band. As described in Sec. IIA, we have employed the relation $p = (\nu/R_H e)_{\eta\eta=K}$ with a constant anisotropy factor of 0.6. In contrast, according to the THE model the relationship between the number of carriers occupying a Cohen surface and R_H should involve an anisotropy factor $\nu(p)$ which varies appreciably with the number of carriers. In particular, over the carrier concentration range involved in our study, ν would vary from approximately 0.3 to 0.7. Thus the two models lead to considerably different values of p for a given sample and, consequently, to markedly different dependences of m_s upon p for a series of such samples. This point has been discussed in detail by THE.

Based upon existing information we have not been able to justify either a constant ν or a carrier-concentration-dependent $\nu(p)$ as applied to a Cohen-type band. It has been established experimentally by Houston *et al.*⁸ that $\nu \sim 0.6$ for SnTe

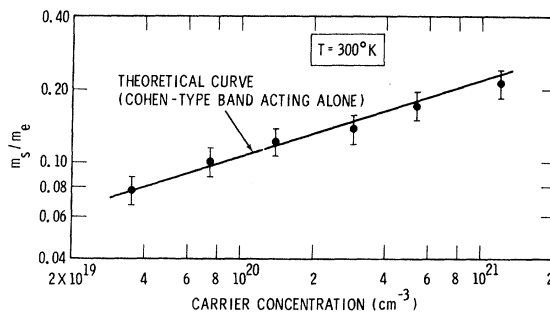


FIG. 6. Comparison of the experimental carrier concentration dependence of the electric-susceptibility hole mass m_s/m_e at 300°K with that expected on the basis of a Cohen-type band acting alone.

over a wide carrier concentration range. THE assert that the constancy of r is the result of the combined contribution of the Cohen band and the second band of their model. On the other hand, Allgaier²² has discussed a way in which Cohen-type surfaces by themselves could lead to a constant r .

Because of the factors discussed above, the good agreement between the simple Cohen model and the experimental data must be considered only as an empirical fact. It is a fact, however, which should be of considerable use in the final determination of the valence-band structure of this material. We believe that similar reservations must also be applied to any comparison of experiment with the THE model.

B. Temperature Dependence

Serious discrepancies exist between experiment and the models discussed above in connection with the temperature dependence of m_s . We have observed a very uniform decrease in m_s as the temperature is lowered, as shown in Fig. 2. The temperature dependences to be expected on the basis of each of the four models cannot be calculated in detail because the variations of their band parameters with temperature are not known. However, the general nature of the changes in m_s which would normally be expected are in sharp contrast to our observations. In particular, one would expect all the models to predict (a) An increase in m_s as the temperature is lowered rather than the observed decrease. This arises from the fact that the valence-conduction-band gap E_g of SnTe has been reported to increase with decreasing temperature. (b) A nonuniform shift of m_s as a function of carrier concentration as the temperature is lowered rather than the very uniform one which is observed. This expectation arises from the fact that multiple bands are involved in three of these models. For such cases, one would generally expect the relative positions and shapes of the bands to change with temperature so as to produce nonuniform shifts in m_s .

Thus, because of the discrepancies discussed above, we feel that none of the models provide a satisfactory description of both the carrier concentration and temperature dependence of m_s .

We wish to emphasize an aspect of our results which should be of considerable significance in future efforts to determine the valence-band struc-

ture of SnTe. As discussed, our measurements show that m_s decreases as the temperature is reduced from 300 to 80° K. The work of others²³ indicates that for such a temperature variation the corresponding forbidden energy gap E_g increases. Such an inverse variation of these quantities is very unusual. To our knowledge there have been no previously reported cases for which the temperature coefficients of m_s and E_g are of a different sign.²⁴ On the basis of this, we consider our results to be anomalous.

The fact that the temperature coefficients of m_s and E_g are normally found to be of the same sign is completely consistent with the results to be expected on the basis of a wide variety of valence-conduction-band models applying to semiconductors. According to such models, m_s would be expected to vary in the same direction as E_g . The anomalous behavior which we observe indicates strongly that the valence-conduction-band structure of SnTe must be characterized by unusual features.

This latter assertion has been supported recently by Burke and Riedl²⁵ who have reported an anomalous behavior of the fundamental absorption edge of SnTe. They observed that the temperature coefficient of the fundamental absorption edge of SnTe in the high-energy region is also opposite in sign to that of E_g . The authors suggested that this anomaly could be explained on the basis of a highly distorted and temperature-dependent Fermi surface. Whether or not such a model can be used to explain our results for m_s is not known. We were not able to carry out a quantitative calculation because their model has not yet been developed in sufficient detail.

VI. SUMMARY

The valence-band models which have been proposed for SnTe by (i) Koehler, (ii) Rogers, and (iii) Tsu, Howard, and Esaki do not provide a satisfactory description of both the temperature and carrier concentration dependence of m_s which we have observed. The same conclusion applies to the simple Cohen-type model which we have considered. In addition, the observed temperature dependence of m_s is found to be anomalous with regard to its relationship to the corresponding variations of the forbidden energy gap. Taken together, these findings suggest that the valence-band structure of SnTe is considerably more complicated than described by any of the models considered here.

†Work constitutes part of a thesis submitted to the University of Maryland, College Park, Md., by R. F. Bis in partial fulfillment of the requirements of the

Ph. D. degree in Physics.

¹B. A. Efimova, V. I. Kaidanov, B. Ya. Maizhes, and I. A. Chernik, Fiz. Tverd. Tela 7, 2524 (1965) [Soviet

- Phys. Solid State 7, 2032 (1966)].
- ²H. Koehler and Z. Angew, Phys. 23, 270 (1967).
- ³L. M. Rogers, J. Phys. D 1, 845 (1968).
- ⁴R. Tsu, W. E. Howard, and L. Esaki, Phys. Rev. 172, 779 (1968).
- ⁵H. R. Riedl, J. R. Dixon, and R. B. Schoolar, Phys. Rev. 162, 692 (1967).
- ⁶B. B. Houston, R. F. Bis, and E. Gubner, Bull. Am. Phys. Soc. 6, 436 (1961).
- ⁷R. F. Brebrick, J. Phys. Chem. Solids 24, 27 (1963).
- ⁸B. B. Houston, R. S. Allgaier, J. Babiskin, and P. G. Siebenmann, Bull. Am. Phys. Soc. 9, 60 (1964).
- ⁹M. K. Norr, J. Electrochem. Soc. 113, 621 (1966).
- ¹⁰R. F. Bis, Ph. D. thesis, University of Maryland, 1969 (unpublished).
- ¹¹H. R. Riedl, R. B. Schoolar, and B. B. Houston, Solid State Commun. 4, 399 (1966).
- ¹²F. Stern, in *Solid State Physics*, edited by F. Seitz and D. Turnbull (Academic, New York, 1963), Vol. 15, p. 344.
- ¹³R. B. Schoolar, H. R. Riedl, and J. R. Dixon, Solid State Commun. 4, 423 (1966).
- ¹⁴R. B. Schoolar and J. R. Dixon, J. Opt. Soc. Am. 58, 119 (1968).
- ¹⁵H. R. Riedl and R. B. Schoolar, Phys. Rev. 131, 2082 (1963).
- ¹⁶Thickness of sample *F* was obtained by private communication with R. B. Schoolar, U.S. Naval Ordnance Lab.
- ¹⁷E. Burstein, Phys. Rev. 93, 632 (1954).
- ¹⁸J. R. Dixon and H. R. Riedl, Phys. Rev. 138, 873 (1965).
- ¹⁹J. N. Zemel, J. D. Jensen, and R. B. Schoolar, Phys. Rev. 140, A330 (1965).
- ²⁰B. B. Houston and R. S. Allgaier, Bull. Am. Phys. Soc. 9, 293 (1964).
- ²¹M. H. Cohen, Phys. Rev. 121, 387 (1961).
- ²²R. S. Allgaier, Phys. Rev. 152, 808 (1966).
- ²³L. Esaki and P. J. Stiles, Phys. Rev. Letters 16, 1108 (1966).
- ²⁴Experimental results reported for GeTe (Ref. 4) suggest the possibility that such an anomaly may exist in this material. However, the evidence is not as clear cut as in the case of SnTe, since the variations of the mass with temperature are considerably smaller and are nonuniform with carrier concentration.
- ²⁵J. R. Burke and H. R. Riedl, Phys. Rev. 184, 830 (1969).

Electron Mobility in Direct-Gap Polar Semiconductors

D. L. Rode

Bell Telephone Laboratories, Murray Hill, New Jersey

(Received 30 March 1970)

The electron drift mobilities of the five direct-gap III-V semiconductors GaAs, GaSb, InP, InAs, and InSb are presented as a function of temperature. Polar-mode, deformation-potential acoustic, and piezoelectric scattering are included, as well as nonparabolic conduction bands and the corresponding electron wave functions. The drift mobility follows exactly from the assumed model by a simple iterative technique of solution which retains all the advantages of variational techniques without, however, the need for excessive mathematical detail. Piezoelectric scattering is shown to be considerable in GaAs for temperatures below 100 °K. The agreement between theory and experiment for GaAs is satisfactory.

I. INTRODUCTION

In recent years, considerable interest has developed toward the study^{1,2} and use^{3,4} of compound semiconductors. The materials about which the most detailed information is available possess direct energy gaps and are derived from elements in columns III and V of the Periodic Table. These semiconductors are five in number: GaAs, GaSb, InP, InAs, and InSb.

Compound semiconductors are peculiarly useful because electron transport at high (but easily achieved) electric fields is dominated by the complex conduction-band structure well above the low-

est band edge.^{5,6} Devices relying on the influence of the higher-energy areas of the conduction band represent a new class of applications (e.g., bulk effects^{7,8}) distinct from that involving energies within a few times the thermal energy of the band edge. Obviously, one now has a wider selection of band structures available, as compared to column-IV semiconductors alone. In addition, the five semiconductors listed above have exhibited some of the highest electron mobilities attained in the liquid-nitrogen to room-temperature range. Hall effect detector devices, of course, operate more efficiently with high mobilities.

The electron mobility is a popular parameter